



All Theses and Dissertations

2015-03-01

Investigation of Laboratory Test Procedures for Assessing the Structural Capacity of Geogrid-Reinforced Aggregate Base Materials

Jaren Tolman Knighton

Brigham Young University - Provo

Follow this and additional works at: <https://scholarsarchive.byu.edu/etd>



Part of the [Civil and Environmental Engineering Commons](#)

BYU ScholarsArchive Citation

Knighton, Jaren Tolman, "Investigation of Laboratory Test Procedures for Assessing the Structural Capacity of Geogrid-Reinforced Aggregate Base Materials" (2015). *All Theses and Dissertations*. 4443.

<https://scholarsarchive.byu.edu/etd/4443>

This Thesis is brought to you for free and open access by BYU ScholarsArchive. It has been accepted for inclusion in All Theses and Dissertations by an authorized administrator of BYU ScholarsArchive. For more information, please contact scholarsarchive@byu.edu, ellen_amatangelo@byu.edu.

Investigation of Laboratory Test Procedures for Assessing the Structural Capacity
of Geogrid-Reinforced Aggregate Base Materials

Jaren Tolman Knighton

A thesis submitted to the faculty of
Brigham Young University
in partial fulfillment of the requirements for the degree of
Master of Science

W. Spencer Guthrie, Chair
Mitsuru Saito
Kevin W. Franke

Department of Civil and Environmental Engineering

Brigham Young University

March 2015

Copyright © 2015 Jaren Tolman Knighton

All Rights Reserved

ABSTRACT

Investigation of Laboratory Test Procedures for Assessing the Structural Capacity of Geogrid-Reinforced Aggregate Base Materials

Jaren Tolman Knighton
Department of Civil and Environmental Engineering, BYU
Master of Science

The modulus of aggregate base layers in pavement structures can potentially be increased through the use of geogrid. However, methods for determining how much structural benefit can be expected from a given geogrid product have not been standardized. A laboratory testing protocol is therefore needed to enable evaluation, in terms of modulus or California bearing ratio (CBR), for example, of the degree of improvement that may be achieved by a given geogrid. Consequently, the objective of this research was to identify a laboratory test method that can be used to quantify improvements in structural capacity of aggregate base materials reinforced with geogrid.

For this research, National Cooperative Highway Research Program Report 598 repeated load triaxial, American Association of State Highway and Transportation Officials (AASHTO) T 307 quick shear, and CBR testing protocols were used to test unreinforced and geogrid-reinforced aggregate base materials from northern Utah. Biaxial and triaxial geogrid were investigated in multiple reinforcement configurations. Several statistical analyses were performed on the results of each test method to identify the test that is most likely to consistently show an improvement in the structural capacity of aggregate base materials reinforced with geogrid.

The results of this research indicate that, for the methods and materials evaluated in this study, calculation of the modulus at 2 percent strain from the AASHTO T 307 quick shear data is the test method most likely to consistently show an improvement in structural capacity associated with geogrid reinforcement. Of the three configurations investigated as part of this research, placing the geogrid at an upper position within a specimen is preferred.

Given that the end goal of the use of geogrid reinforcement is to improve pavement performance, additional research is needed to compare the results of the AASHTO T 307 quick shear test obtained in the laboratory with the structural capacity of geogrid-reinforced aggregate base materials measured in the field. In addition, correlations between the results of the AASHTO T 307 quick shear test and resilient modulus need to be investigated in order to incorporate the findings of the AASHTO T 307 quick shear test on reinforced base materials into mechanistic-empirical pavement design.

Key words: aggregate base materials, biaxial geogrid, mechanistic-empirical pavement design, modulus, quick shear test, triaxial geogrid

ACKNOWLEDGEMENTS

This research was funded by the Utah Department of Transportation. I thank Staker Parson Companies, Geneva Rock Products, and Tensar International Corporation for supplying the materials used in this research. I acknowledge the contributions of Brigham Young University students Jake Tolbert and Kirk Jackson in completing this research. I appreciate Dr. Mitsuru Saito and Dr. Kevin W. Franke for participating on my graduate advisory committee and Dr. Dennis L. Eggett for his assistance and guidance in completing the statistical analyses included in this research. I am especially grateful to Dr. W. Spencer Guthrie for his mentorship, friendship, and example; my interactions with him have made me a better student, researcher, and person. Most importantly, I thank my wife, Cheri, for her devotion and encouragement throughout my graduate work. My success and accomplishments are because of her love and support.

TABLE OF CONTENTS

LIST OF TABLES	vi
LIST OF FIGURES	vii
1 INTRODUCTION	1
1.1 Problem Statement	1
1.2 Research Objective and Scope	3
1.3 Outline of Report.....	3
2 BACKGROUND	5
2.1 Overview	5
2.2 Pavement Design and Construction	5
2.3 Geogrid Reinforcement	6
2.3.1 Laboratory Testing.....	6
2.3.2 Field Testing	10
2.4 Summary	12
3 PROCEDURES	13
3.1 Overview	13
3.2 Experimental Design	13
3.3 Materials Characterization	18
3.4 Testing of Geogrid-Reinforced Base Materials	18

3.4.1	NCHRP Report 598 RLT Testing.....	18
3.4.2	AASHTO T 307 Quick Shear Testing.....	23
3.4.3	California Bearing Ratio Testing.....	25
3.5	Statistical Analyses	26
3.6	Summary	28
4	RESULTS AND ANALYSIS	31
4.1	Overview	31
4.2	Test Results	31
4.3	Statistical Analyses	34
4.4	Summary	44
5	CONCLUSION	47
5.1	Summary	47
5.2	Findings.....	48
5.3	Recommendations.....	48
	REFERENCES	51
	APPENDIX A MOISTURE-DENSITY RELATIONSHIPS	55
	APPENDIX B MECHANICAL PROPERTY TEST DATA	57
	APPENDIX C ANOCOVA RESULTS.....	61
	APPENDIX D POST-HOC PAIRWISE COMPARISONS	63

LIST OF TABLES

Table 3-1: Experimental Design	14
Table 4-1: Moisture-Density Relationships	32
Table 4-2: NCHRP Report 598 RLT Test Results.....	33
Table 4-3: AASHTO T 307 Quick Shear Test Results.....	34
Table 4-4: CBR Test Results	34
Table 4-5: Statistical Analyses of NCHRP Report 598 RLT Test Results.....	35
Table 4-6: Statistical Analyses of AASHTO T 307 Quick Shear Test Results	36
Table 4-7: Statistical Analyses of CBR Test Results.....	36
Table 4-8: Lower Bounds for AASHTO T 307 Methods of Data Analysis	38
Table 4-9: Lower Bounds for AASHTO T 307 Geogrid Configurations.....	38
Table B-1: NCHRP Report 598 RLT Test Data	58
Table B-2: AASHTO T 307 Quick Shear Test Data	59
Table B-3: CBR Test Data	60
Table C-1: Full ANOCOVA Models.....	62
Table C-2: Reduced ANOCOVA Models	62
Table D-1: Post-Hoc Comparison of Means.....	63

LIST OF FIGURES

Figure 1-1: Examples of (a) biaxial and (b) triaxial geogrid.	2
Figure 3-1: Point of the Mountain aggregate base material.....	15
Figure 3-2: Trenton aggregate base material.	15
Figure 3-3: Testing configurations for NCHRP Report 598 RLT and AASHTO T 307 quick shear testing.....	17
Figure 3-4: Testing configuration for CBR testing.....	17
Figure 3-5: UTM-100 testing equipment.....	19
Figure 3-6: Steel split mold for compacting specimens.....	20
Figure 3-7: Membrane expander.....	22
Figure 3-8: Triaxial cell placed inside the UTM-100.....	23
Figure 3-9: CBR specimen placed inside the Instron material testing machine.....	26
Figure 4-1: Particle-size distributions.....	32
Figure 4-2: Typical Point of the Mountain specimens after AASHTO T 307 quick shear testing: (a) no geogrid, (b) geogrid configuration A, (c) geogrid configuration B, (d) geogrid configuration C.	40
Figure 4-3: Typical Trenton specimens after AASHTO T 307 quick shear testing: (a) no geogrid, (b) geogrid configuration A, (c) geogrid configuration B, (d) geogrid configuration C.	41
Figure 4-4: Modulus values for AASHTO T 307 quick shear testing in geogrid configuration A.....	43
Figure 4-5: Modulus values for AASHTO T 307 quick shear testing in geogrid configuration B.	43
Figure 4-6: Modulus values for AASHTO T 307 quick shear testing in geogrid configuration C.	44
Figure A-1: Moisture-density curve for Point of the Mountain material.....	55
Figure A-2: Moisture-density curve for Trenton material.....	56

1 INTRODUCTION

1.1 Problem Statement

Flexible pavements are generally designed to have multiple layers, including the asphalt surface course, aggregate base course, and native subgrade. In pavement design, engineers need to know the structural properties of each layer in order to determine thicknesses of the asphalt and aggregate base layers. For aggregate base materials, structural capacity is commonly quantified in terms of modulus or California bearing ratio (CBR), for example, with the former being an especially important input in the Mechanistic-Empirical Pavement Design Guide (MEPDG) (AASHTO 2008, NCHRP 2004a, NHI 2002). The modulus of aggregate base layers can potentially be increased through the use of geogrid, an extruded polypropylene material, which would then enable reductions in base layer thickness (Montanelli et al. 1997, Cancelli and Montanelli 1999) or prolonged service life (Al-Qadi et al. 1997, Cancelli and Montanelli 1999) compared to unreinforced sections.

Geogrid is available globally in different geometries from several different manufacturers, with two primary examples shown in Figure 1-1. Manufactured in wide rolls, geogrid is generally placed directly on prepared subgrade soils and covered with aggregate base material that is compacted in place (Montanelli et al. 1997). To the extent that the aggregate particles penetrate the openings, or apertures, in the geogrid, the geogrid increases the lateral confinement of the base material in the region around the geogrid (Al-Qadi et al. 2008, Qian et

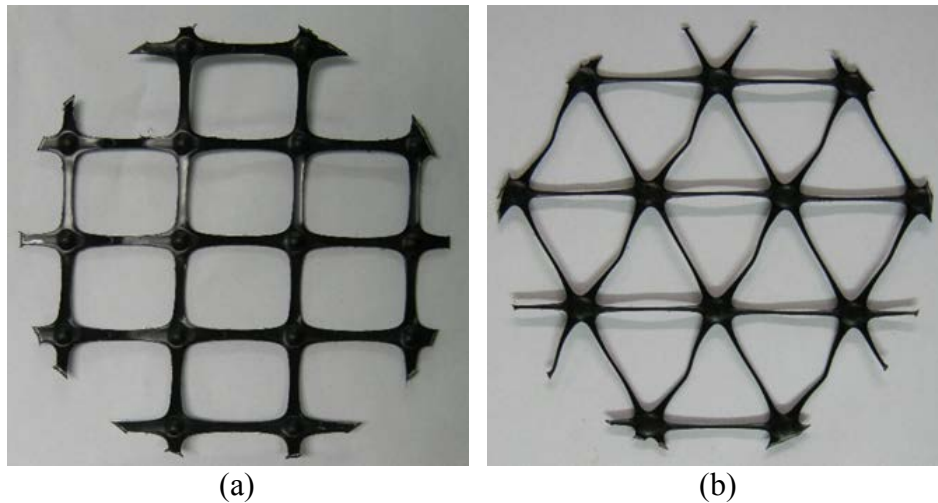


Figure 1-1: Examples of (a) biaxial and (b) triaxial geogrid.

al. 2013), which can result in an increase in the modulus of the base layer (Kwon et. al 2008, Perkins and Ismeik 1997, Perkins 1999). In this way, the degree of improvement in modulus is determined by the extent of interlock that occurs between the aggregate and the geogrid; for this reason, geogrid properties such as rib size, aperture size, aperture shape, material type, and tensile strength can influence the interlock that occurs with a given base material (Hatami et al. 2012, Tutumluer and Kwon 2006). However, methods for determining how much structural benefit can be expected from a given geogrid product have not been standardized. Although a pull-out test has been used to evaluate the extent of interlock of a given geogrid product with a given soil (Hatami et al. 2012, Palmeira 2004), that test does not generate results that can be used in pavement design. A laboratory testing protocol is therefore needed to enable evaluation, in terms of modulus or CBR, for example, of the degree of improvement that may be achieved by a given geogrid so that the cost of incorporating the geogrid in a pavement structure can be compared with the potential cost savings associated with its use.

1.2 Research Objective and Scope

The objective of this research, which was commissioned by the Utah Department of Transportation (UDOT), was to identify a laboratory test method that can be used to quantify improvements in structural capacity of aggregate base materials reinforced with geogrid. The scope of this research involved two aggregate base materials commonly selected for pavement construction on UDOT projects; two types of geogrid, including biaxial (BX) and triaxial (TX); and three laboratory test methods. Specifically, the laboratory test methods included the repeated load triaxial (RLT) test described in Appendix B of the National Cooperative Highway Research Program (NCHRP) Report 598 entitled “Proposed Standard Test Method for Shear Strength of Aggregate by the Repeated Load Triaxial Test” (NCHRP 2004b), which was specifically requested by UDOT engineers for this research; the quick shear portion of American Association of State Highway and Transportation Officials (AASHTO) T 307 (Determining the Resilient Modulus of Soils and Aggregate Materials); and the CBR test described in American Society for Testing and Materials (ASTM) D1883 (Standard Test Method for CBR (California Bearing Ratio) of Laboratory-Compacted Soils). For testing using the NCHRP Report 598 RLT and AASHTO T 307 quick shear methods, geogrid position, or configuration, within the aggregate specimens was also investigated; all unique combinations of geogrid type and configuration were evaluated in this research for comparison with unreinforced specimens that were used as controls.

1.3 Outline of Report

This report contains five chapters. This chapter introduces the research by presenting the problem statement, research objectives, and scope. Chapter 2 gives background information on geogrid reinforcement of base materials in flexible pavements. Chapters 3 and 4 detail the

procedures and results, respectively, of the research. Chapter 5 provides conclusions and recommendations resulting from the research.

2 BACKGROUND

2.1 Overview

This chapter discusses pavement design and construction and describes geogrid reinforcement in the context of both laboratory and field testing of aggregate base materials.

2.2 Pavement Design and Construction

Flexible pavements are generally designed to have multiple layers of varying mechanical properties, with stronger layers placed over weaker layers. The surface course in a flexible pavement structure is normally a hot mix asphalt layer. Having a comparatively high modulus, the asphalt protects the underlying base course and subgrade by decreasing the magnitude of traffic-induced stresses that are transferred downwards into the pavement structure.

The base course is normally composed of a dense-graded aggregate base material, which provides additional protection to the underlying subgrade. Traffic loads are distributed through the base layer through interparticle friction between aggregates (Kwon and Tutumluer 2009, Xiao et al. 2012). As the aggregate base material is compacted in place to a specified density, the resulting interparticle friction between especially the larger aggregates allows the base layer to spread traffic loads over the subgrade.

The subgrade is the natural soil that exists on a site and may exhibit very low modulus values. In particular, weak subgrade materials can cause difficulty in road construction because

they may not offer sufficient support for compaction of overlying base materials to an appropriate density. For this reason, geogrid reinforcement is sometimes placed over weak subgrades to potentially create an improved construction platform that leads to better compaction and greater strength of the base material (Tutumluer and Kwon 2006, Wayne et al. 2011a).

2.3 Geogrid Reinforcement

Since the 1980s, geogrid reinforcement of base materials has been increasingly used in roadway construction (Montanelli et al. 1997, Perkins 1999, Tutumluer et al. 2009), and several studies have been performed to evaluate its performance. The results of both laboratory and field testing are summarized in the following sections.

2.3.1 Laboratory Testing

Numerous laboratory experiments have been performed to better understand geogrid reinforcement of aggregate base material. The experiments involved evaluation of modulus and permanent deformation as measured in the plate load test, triaxial shear test, and RLT test.

Cyclic plate load testing involves compressive loading of a circular plate and measurement of the surface deflection of the supporting material as described in ASTM D1195 (Standard Test Method for Repetitive Static Plate Load Tests of Soils and Flexible Pavement Components, for Use in Evaluation and Design of Airport and Highway Pavements). The results of cyclic plate load tests on laboratory-scale pavement sections with a crushed limestone aggregate base were analyzed using the MEPDG in one study, and the researchers concluded that geogrid reinforcement increased the resilient modulus of the base materials by 10 to 90 percent and suggested that the base layer thickness could therefore be decreased by up to 49 percent (Chen and Abu-Farsakh 2012); in this study, geogrid was placed at one of three locations,

including the base-subgrade interface, the middle of the base layer, or the upper one-third position within the base layer in the reinforced sections, which were composed of a 12-in.-thick base layer and a 0.75-in.-thick asphalt layer. However, in another study, cyclic plate load tests performed on crushed base material composed of reclaimed asphalt pavement (RAP) and recycled concrete aggregate (RCA) showed that, while permanent deformation was significantly different for the unreinforced and reinforced materials, the resilient modulus did not increase significantly for the reinforced sections (Wayne et al. 2011b); in this study, geogrid was placed at the middle of the base layer in the reinforced sections, which were composed of a 12-in.-thick base layer. One study performed on a dense-graded aggregate base layer focused on evaluating correlations between various geogrid index properties, such as junction and rib strength and pullout resistance, and the results of plate load tests indicated that the change in stiffness achieved for a given aggregate base material depended on the properties of the geogrid (Hatami et al. 2012); in this study, geogrid was placed at one of three locations, including the base-subgrade interface, 1 in. above a geotextile that was placed at the base-subgrade interface, or directly on top of a geotextile that was placed at the base-subgrade interface in the reinforced sections, which each had an 8-in.-thick base layer. The results of plate load testing performed on laboratory-scale pavement sections with a crushed-stone aggregate base indicated that the same pavement life can be achieved with a base thickness that is reduced by up to 20 percent as a result of the inclusion of geogrid (Perkins 1999); in this study, geogrid was placed at one of two locations, including the base-subgrade interface or the lower one-third position within the base layer in the reinforced sections, which each had a base layer that varied in thickness from 8 to 15 in. and an asphalt layer that was 3 in. thick. In a modified plate load test performed in a study specific to railway track structures, cyclic loading in a box was performed on ballast material;

this research showed that there was an optimum geogrid aperture size for a given nominal aggregate size (Brown et al. 2007); in this study, geogrid was placed at one of two locations, including the ballast-subballast interface or 2 in. above the ballast-subballast interface in the reinforced sections, which each had a 12-in.-thick base layer.

Triaxial shear testing involves compressive loading of a confined cylindrical test specimen at a constant vertical strain rate and measurement of the load sustained by the specimen during the testing as described in ASTM D7181 (Method for Consolidated Drained Triaxial Compression Test for Soils). In one study, triaxial shear testing performed at a rate of 10 percent strain per hour on crushed limestone samples showed that the strength and stiffness of geogrid-reinforced samples were higher than those of unreinforced samples and that greater improvement from geogrid was realized at higher strain levels (Nazzal et al. 2007); in this study, geogrid was placed at one of three locations, including the middle, upper one-third, or upper and lower one-third positions within the reinforced specimens, which were 6 in. in diameter and 12 in. in height.

RLT testing involves compressive loading of a confined cylindrical test specimen in repeated load pulses followed by rest periods as described in NCHRP Report 598 (NCHRP 2004b) or AASHTO T 307. Multiple studies using RLT testing to investigate the permanent deformation and resilient modulus of geogrid-reinforced samples have found that geogrid reinforcement reduced permanent deformation but did not significantly increase resilient modulus (Abu-Farsakh et al. 2012, Moghaddas-Nejad and Small 2003, Nazzal et al. 2007, Perkins et al. 2004, Wayne et al. 2011b); in these studies, “common” crushed aggregate, crushed limestone aggregate, finely crushed basaltic aggregate, and RAP with RCA were evaluated with geogrid placed at the middle, lower one-third, upper one-third, and/or upper and lower one-third

positions within the reinforced specimens, which were either 6 in. in diameter and 12 in. in height, 9 in. in diameter and 18 in. in height, or 12 in. in diameter and 24 in. in height. However, another study that used RLT testing to evaluate RAP, RCA, and crushed brick indicated that the permanent deformation not only decreased by up to 37 percent but that the resilient modulus also increased by up to 55 percent for geogrid-reinforced specimens compared to unreinforced specimens (Rahman et al. 2014); in this study, geogrid was positioned at the middle of the reinforced specimens, which were 4 in. in diameter and 8 in. in height. Another study reported that specimens with a higher density above the geogrid, simulating the higher density possible because of the reinforcing effects of geogrid, exhibited a significant increase in resilient modulus when compared to unreinforced specimens (Wayne et al. 2011a); in this study, geogrid was placed at the middle of the reinforced specimens, which were 6 in. in diameter and 12 in. in height. In another study, RLT testing performed on crushed amphibolite showed that geogrid confines a region that extends approximately one specimen diameter above and below the geogrid (Perkins et al. 2004); in this study, geogrid was placed at the middle of the reinforced specimens, which were 12 in. in diameter and 24 in. in height. Another laboratory study utilized RLT testing to investigate the effect of varying geogrid position, geometry, and tensile properties on the structural capacity of aggregate base materials and found that the location of the geogrid within the test specimens contributed most to the reduction in permanent strain in the specimens and that placing the geogrid at the upper one-third position within the specimen yielded better results than placing the geogrid at the middle of the specimen (Abu-Farsakh et al. 2012); in this study, geogrid was placed at one of three locations, including the middle, upper one-third, or upper and lower one-third positions within the reinforced specimens, which were 6 in. in diameter and 12 in. in height. Other studies have also concluded that varying the location of

geogrid within specimens or laboratory-scale pavement sections can have a significant effect on test results (Chen and Abu-Farsakh 2012, Nazzal et al. 2007); nonetheless, as demonstrated in most of the cited studies, placing the geogrid at the middle is most common.

2.3.2 *Field Testing*

Numerous field experiments have been performed to better understand geogrid reinforcement of aggregate base material. The experiments involved evaluation of pavement responses and properties, including cracking, rutting, and stiffness as measured in distress surveys and dynamic cone penetrometer (DCP) tests.

Distress surveys involve assessing the distresses, including cracking and rutting, evident in a pavement section. Distress surveys are commonly performed after accelerated pavement testing and full-scale field testing to evaluate pavement performance. Full-scale field testing involves constructing pavement sections and subjecting them to trafficking, usually in a controlled environment, and accelerated pavement testing involves subjecting pavement sections to specified levels of trafficking in a comparatively short period of time, usually using a testing assembly. A study performed using full-scale accelerated pavement testing with measurements of rutting and cracking showed that placing the geogrid at the base-subgrade interface was best for thin aggregate base layers, while placing the geogrid within the base layer was best for thicker base layers (Al-Qadi et al. 2008); in this study, geogrid was placed at one of two locations, including the base-subgrade interface or the upper one-third position within the base layer in the reinforced sections, which each had a base layer that varied in thickness from 8 to 18 in. Another study performed using accelerated pavement testing on a one-third-scale model pavement section found that the resilient modulus of the pavement section was not significantly influenced by the inclusion of geogrid reinforcement, but rutting in the subgrade layer was

reduced (Tang et al. 2013); in this study, geogrid was placed at the base-subgrade interface in the reinforced sections, which each had a 4-in.-thick base layer and a 1.5-in.-thick asphalt layer. In one study, researchers constructed a single-lane test track with different types of geogrid in many test sections with base thickness varying from 12 to 20 in. throughout the track; they found that 12-in.-thick geogrid-reinforced base layers sustained the same amount of rutting as 20-in.-thick unreinforced base layers (Cancelli and Montanelli 1999); in this study, geogrid was placed at the base-subgrade interface in the reinforced sections, which each had a base layer that varied in thickness from 12 to 20 in. and a 3-in.-thick asphalt layer.

DCP testing involves recording the number of hammer drops required to drive a cone-tipped rod into the ground, and the penetration rate of the rod is used to estimate the in-situ strength of soils as described in ASTM D6951 (Standard Test Method for Use of the Dynamic Cone Penetrometer in Shallow Pavement Applications). In one study, DCP test results showed that a region of increased stiffness immediately above the geogrid layer was attained because of the lateral confinement provided by the geogrid (Kwon et al. 2008); in this study, geogrid was placed at one of two locations, including the base-subgrade interface or the lower one-third position within the base layer in the reinforced section, which had a base layer that varied in thickness from 8 to 18 in. and an asphalt layer that was 3 in. thick. In another study, the results of DCP tests performed on unreinforced and geogrid-reinforced pavement sections after 5 years of trafficking showed that the reinforced base materials had a region extending 4 to 6 in. above the geogrid with increased stiffness when compared to the unreinforced materials (Kwon and Tutumluer 2009); in this study, geogrid was placed at the base-subgrade interface in the reinforced sections, which each had a base layer that varied in thickness from 6 to 11 in. and an asphalt layer that was 9 to 11 in. thick.

2.4 Summary

Flexible pavements are generally designed to have multiple layers of varying mechanical properties, with stronger layers placed over weaker layers. The layers normally included in flexible pavement are a surface course composed of hot mix asphalt, a base course composed of aggregate base material, and the natural soil that exists on site, known as the subgrade. Each layer protects the layers beneath by decreasing the magnitude of traffic-induced stresses that are transferred downwards into the pavement structure. The interparticle friction in the base course, especially between the larger aggregates, allows the base layer to spread traffic loads over the subgrade. Weak subgrade materials can cause difficulty in road construction because they may not offer sufficient support for compaction of overlying base materials to an appropriate density. Geogrid reinforcement is sometimes placed over weak subgrades to create an improved construction platform that leads to better compaction and greater strength of the base material.

Since the 1980s, geogrid reinforcement of base materials has been increasingly used in roadway construction, and several laboratory and field studies have been performed to evaluate its performance. Laboratory testing has involved evaluation of a number of material properties as measured in the plate load test, triaxial shear test, and RLT test. Field testing has involved evaluation of pavement responses and properties as measured in distress surveys and DCP tests. Multiple laboratory studies have shown increases in modulus as a result of geogrid reinforcement, while other studies have not shown an increase. Likewise, some field studies have shown increases in modulus and stiffness as a result of geogrid reinforcement, while other studies have not shown an increase. Variations in testing protocols, specimen dimensions, materials, and geogrid placement may all contribute to the inconsistent results of these laboratory and field studies on geogrid reinforcement of aggregate base materials.

3 PROCEDURES

3.1 Overview

This research was motivated by the need to identify a single laboratory test protocol that UDOT engineers could specify to quantify improvements in structural capacity of aggregate base materials reinforced with geogrid. In this research, various laboratory testing procedures were evaluated with respect to their ability to demonstrate improvements in material properties commonly used in pavement design, such as modulus or CBR, for example. This chapter describes the experimental design, materials characterization, test procedures, and statistical analyses performed for this research.

3.2 Experimental Design

The experimental design for this research is presented in Table 3-1. Testing was performed on aggregate base materials from the Point of the Mountain Pit and the Trenton Gravel Pit #3, both of which are located in northern Utah. The base materials from the Point of the Mountain and Trenton Pits were included in this research because they are representative of aggregate base materials commonly used on UDOT projects and because they also exhibit different particle angularity; as depicted in Figures 3-1 and 3-2, the Point of the Mountain material is an angular, crushed aggregate, and the Trenton material is a rounded gravel. In addition to unreinforced control specimens, testing was also performed on specimens reinforced

Table 3-1: Experimental Design

Material	Geogrid Type	Geogrid Configuration	Test Protocol			
			NCHRP 598	AASHTO T 307	CBR	
Point of the Mountain	None	-	x	x	x	
		A	x	x	x	
		B	x	x		
	BX	C	x	x		
		TX	A	x	x	x
			B	x	x	
	C		x	x		
	Trenton	None	-	x	x	x
			A	x	x	x
B			x	x		
TX		C	x	x		
		A	x	x	x	
		B	x	x		
		C	x	x		

with BX or TX geogrid, which was supplied in rolls by the manufacturer. The purpose of including these primary geogrid types was to ensure that the experimentation was representative of the geogrid products available in the industry. Geogrid circles having a diameter of approximately 5.8 in., as shown in Figure 1-1, were cut from the rolls and placed within the specimens. The geogrid circles were cut in such a way as to preserve the maximum number of intact apertures; the BX geogrid had eight intact rectangular apertures with side lengths of approximately 1.1 and 1.3 in., and the TX geogrid had 13 intact triangular apertures with equal side lengths of approximately 1.5 in. Three different reinforcement configurations were tested for each unique combination of aggregate and geogrid using the NCHRP Report 598 RLT and AASHTO T 307 quick shear test protocols to investigate the effect of geogrid positioning within the aggregate specimen; the three testing configurations A, B, and C are shown in Figure 3-3. As



Figure 3-1: Point of the Mountain aggregate base material.



Figure 3-2: Trenton aggregate base material.

shown in Figure 3-4, only one reinforcement configuration was used in CBR testing due to the reduced height of the specimens. Two replicates of each configuration were tested to allow for statistical analyses of the results.

Different compaction procedures were used for the different reinforcement configurations evaluated in the NCHRP Report 598 and AASHTO T 307 protocols. In configuration A, the geogrid was placed horizontally in the middle of the third of five lifts to allow both top-down and bottom-up penetration of the aggregate into the geogrid apertures. Half of the material for the third lift was placed in the mold and leveled by hand, the geogrid was placed on top, and the second half of the lift was then placed and compacted. In configuration B, the geogrid was placed on top of the third of six lifts to allow top-down penetration of the aggregate. After the third lift was compacted, the surface was lightly scarified, the geogrid was placed on top, and the fourth lift was placed and compacted. In configuration C, the geogrid was placed on top of the sixth of eight lifts after the surface of the sixth lift was scarified in the same manner as performed for configuration B. Configuration C was added to the experimental design to examine placement of geogrid at an upper position within the reinforced specimens. The unreinforced control specimens tested using the NCHRP Report 598 and AASHTO T 307 protocols were compacted in five and six lifts, respectively.

For the CBR testing, the geogrid in configuration A was placed on top of the third of five lifts after the surface of the third lift was lightly scarified. This geogrid position was chosen because it was high enough in the specimen to allow the aggregate to engage the geogrid as the piston was driven into the top of the specimen but also low enough in the specimen to allow development of a normal aggregate matrix above the geogrid. The unreinforced control specimens tested using the CBR testing protocols were compacted in five lifts.

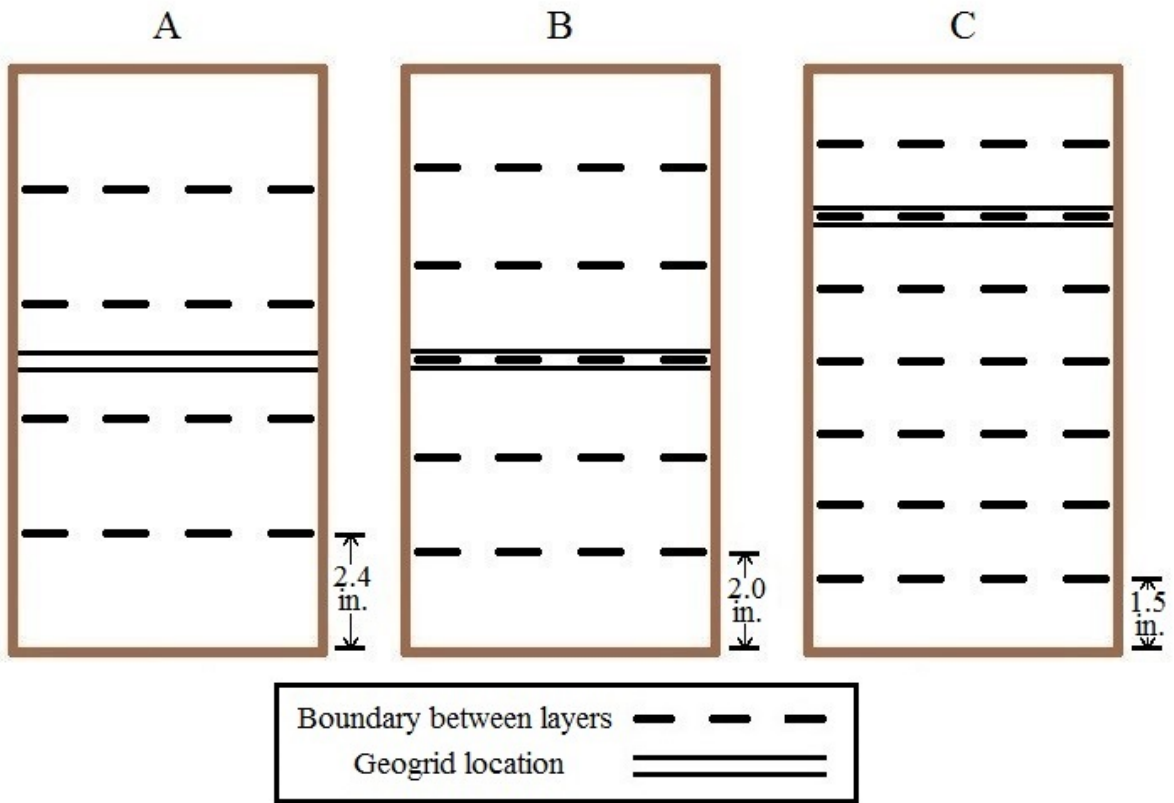


Figure 3-3: Testing configurations for NCHRP Report 598 RLT and AASHTO T 307 quick shear testing.

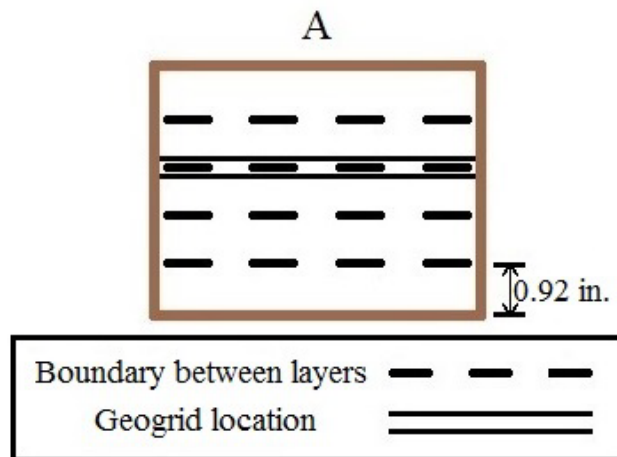


Figure 3-4: Testing configuration for CBR testing.

3.3 Materials Characterization

To characterize the materials, the aggregates were initially dried at 140°F and sieved in bulk to produce a master gradation. Based on the master gradation, samples of each aggregate base material were subsequently prepared for washed sieve analysis, Atterberg limits testing, and determination of optimum moisture content (OMC) and maximum dry density (MDD). In addition, the aggregates were classified according to the Unified Soil Classification System (USCS) and the AASHTO methods. The specific procedures applicable to this testing are documented in other research (Jackson 2015).

3.4 Testing of Geogrid-Reinforced Base Materials

As previously discussed, specimens of geogrid-reinforced aggregate base materials were evaluated using three different methods, including the NCHRP Report 598 RLT, AASHTO T 307 quick shear, and CBR protocols. The specimen preparation and testing procedures are outlined in the following sections.

3.4.1 NCHRP Report 598 RLT Testing

RLT testing was performed in general accordance with the NCHRP Report 598 RLT test procedures. The testing consists of 10 sequences of 1,000 cycles each, where each cycle lasts 1 second. During each cycle, a deviatoric stress is applied through a haversine-shaped load pulse over a 0.1-second time interval that is followed immediately by a 0.9-second rest period. The confining stress remains constant at 15 psi during the test. The deviatoric stress is 10 psi for the first sequence and 20 psi for the second sequence and then increases by 20 psi for each subsequent sequence.

NCHRP Report 598 test procedures require a sophisticated testing apparatus in order to execute the precise loadings and measurements necessary for successful test results. The computer-controlled, servo-hydraulic UTM-100 equipment available in the Brigham Young University Highway Materials Laboratory was utilized for the testing. Figure 3-5 displays the UTM-100 setup in the laboratory.

The specimens prepared for testing using the NCHRP Report 598 method were 6 in. in diameter and 12 in. in height. The appropriate amounts of each sieve size were weighed out for each material according to the respective master gradation to produce a sample of the appropriate dimensions and the target unit weight as determined from the respective MDD.

After being weighed out, the aggregate samples were placed in the oven at 140°F for at least 24 hours to remove any residual moisture. The samples were then removed from the oven,



Figure 3-5: UTM-100 testing equipment.

covered in aluminum foil, and placed on the bench for 4 hours to cool to room temperature. Once the samples were cooled, an appropriate amount of deionized water was added to bring the gravimetric water content of the specimens to 0.5 to 1.0 percent above the previously determined OMC; the additional water was added to compensate for the amount of water evaporation that can occur during sample preparation in the laboratory. The water was mixed into the aggregate samples until uniform color and texture were achieved. The moistened aggregates were then sealed in an airtight plastic bag and allowed to equilibrate for 24 hours.

The specimens were compacted in a custom-made steel split mold with an inner diameter of 6 in. and a height of 12 in., which was fastened to a steel base plate as shown in Figure 3-6. The mold was prepared by first placing a layer of aluminum foil on the base plate to provide support to the bottom of the compacted specimen when it was later transferred from the base



Figure 3-6: Steel split mold for compacting specimens.

plate. A latex membrane was placed inside the mold. The mold was secured to the base plate, and a collar was placed on top of the mold to prevent damage to the top of the inner membrane during the compaction process. Specimens were compacted manually in lifts of equal weight in general accordance with ASTM D1557 (Standard Test Methods for Laboratory Compaction Characteristics of Soil Using Modified Effort (56,000 ft-lbf/ft³ (2,700 kN-m/m³))). Modified Proctor compaction effort required 122 blows per lift for the six-lift specimens, 146 blows per lift for the five-lift specimens, and 92 blows per lift for the eight-lift specimens. Prior to placement of another lift in the mold, a flathead screwdriver was used to lightly scarify the surface of each compacted lift to a depth of about 0.125 in. in three parallel lines, which were 1.5 to 2.0 in. apart, and another three similarly spaced parallel lines perpendicular to the first three. Care was taken not to dislodge large aggregates during this process. A finishing tool was used to flatten the top lift of the specimens; in this process, three drops of a 10-lb. hammer were applied from a height of 18 in. onto a 6-in.-diameter plate placed on top of the compacted specimen. After compaction of a specimen was complete, the specimen and mold were removed from the base plate and placed on top of a saturated, 2-in.-thick, 6-in.-diameter porous stone. The specimen was then removed from the mold, and another saturated porous stone was placed on top of the specimen. A second membrane was placed around the specimen using a membrane expander as shown in Figure 3-7, and the specimen and porous stones were sealed in an airtight plastic bag and left to equilibrate at room temperature for 16 to 24 hours.

When a specimen was ready for placement in the triaxial cell, a saturated, 0.5-in. thick, 6-in.-diameter porous bronze disk was placed on top of the 6-in.-diameter lower metal platen within the triaxial cell. The upper porous stone was removed from the specimen, and the specimen was then moved off the lower porous stone and placed on top of the porous disk.



Figure 3-7: Membrane expander.

Another identical porous bronze disk and 6-in.-diameter metal platen were placed on top of the specimen. Rubber O-rings were used to create an airtight seal between the metal platens and membranes. The top of the triaxial cell was then bolted in place over the specimen, and the entire apparatus was placed into the UTM-100 as shown in Figure 3-8. During testing, a pressure transducer was used to measure the air pressure inside the triaxial cell, and a hole in the center of the lower platen allowed water to drain freely from the specimen.

The resilient modulus and number of cycles to failure were recorded for each specimen tested. (Although cycles to failure is not a pavement design input and would therefore not by itself be an appropriate measure of the degree of improvement that may be achieved by a given geogrid in the context of this research, it was included in this experimentation because it was easy to measure in conjunction with resilient modulus.) As specified in the NCHRP Report 598 test procedures, the resilient modulus was calculated using the methods outlined in the AASHTO



Figure 3-8: Triaxial cell placed inside the UTM-100.

T 307 test procedures. The testing stopped when the specimens reached 10 percent strain or 10,000 cycles, whichever occurred first. After the testing, the specimens were dried to constant weight, and the gravimetric moisture content was calculated. The dry density of each specimen was estimated from the wet density measured immediately after compaction and the moisture content measured immediately after testing.

3.4.2 AASHTO T 307 Quick Shear Testing

Quick shear testing was performed in general accordance with the applicable portions of AASHTO T 307. The specimens were subjected only to the shear portion of the test; the conditioning and resilient modulus portions of the test were not performed. The testing consisted of measuring the compressive load while subjecting the specimens to a constant strain rate of

0.12 in. per minute, which corresponds to 1 percent strain per minute. The confining pressure remained constant at 5 psi throughout the testing.

Specimens tested using the AASHTO T 307 quick shear procedure were prepared in the same manner as the specimens tested using the NCHRP Report 598 method, including the compaction procedures and assembly in the UTM-100. However, in the AASHTO T 307 testing, the specimens were allowed to equilibrate for several minutes until reaching constant height under the applied confining pressure before the testing commenced. Measurements of load and axial displacement were recorded and used to develop a stress-strain plot for each specimen tested. The test stopped when the specimens reached 15 percent strain, and the peak axial stress was recorded. In addition, various modulus values were calculated from the plot, including the modulus to the peak axial stress, the modulus of the elastic portion of the curve, and the modulus at 2 percent strain in the specimens.

The modulus to the peak axial stress was calculated by dividing the peak stress by the corresponding strain. The modulus of the elastic portion of the curve was calculated as the slope of a linear trend line computed for a middle portion of the stress-strain curve between the start of the test and the greater of the peak stress or the stress corresponding to a level of 10 percent strain; specifically, the curve in this range was divided into four segments of equal length, and the slope of the second segment was analyzed. A maximum strain value of 10 percent was chosen in this analysis because all of the specimens experienced plastic deformation at this strain level. The modulus at 2 percent strain was calculated by dividing the stress corresponding to 2 percent strain by a strain value of 2 percent. Linear interpolation was used when necessary to determine the exact value of stress corresponding to 2 percent strain in each test.

After the testing, the specimens were dried to constant weight, and the gravimetric moisture content was calculated. The dry density of each specimen was estimated from the wet density measured immediately after compaction and the moisture content measured immediately after testing.

3.4.3 California Bearing Ratio Testing

CBR testing was performed in general accordance with ASTM D1883. The testing consists of measuring the compressive load sustained by the specimen as a 1.95-in.-diameter loading piston is driven into the top of the specimen at a strain rate of 0.05 in. per minute. Load measurements are reported at every 0.1 in. of penetration up to 0.5 in.

CBR specimens were prepared in much the same way as the specimens tested using the NCHRP Report 598 method; however, the aggregate was compacted into a 6-in.-diameter mold that was only 4.59 in. in height, and latex membranes were not used. Each specimen was compacted using 56 blows per lift in five equal lifts by weight, in general accordance with ASTM D1557. The compacted specimen, mold, and base plate were then sealed in an airtight plastic bag and left to equilibrate at room temperature for 16 to 24 hours, after which the specimen was tested using an Instron material testing machine, as shown in Figure 3-9. A ring-shaped metal weight was placed on top of the specimen to provide the overburden stress required during testing. To calculate the CBR, the stresses computed at the penetration depths of 0.1, 0.2, 0.3, 0.4, and 0.5 in. were divided by 1000, 1500, 1900, 2300, and 2600 psi, respectively, to obtain the ratio of the measured stress to the standard stress. The maximum of these ratios was multiplied by 100 to obtain the CBR. After the testing, the specimens were dried to constant weight, and the gravimetric moisture content was calculated. The dry density of each specimen



Figure 3-9: CBR specimen placed inside the Instron material testing machine.

was estimated from the wet density measured immediately after compaction and the moisture content measured immediately after testing.

3.5 Statistical Analyses

An analysis of covariance (ANOCOVA) was performed on the results of each test for each aggregate base material. The independent variable in each ANOCOVA model was treatment, where an individual treatment was one of seven unique combinations of geogrid type and configuration, as applicable, for the NCHRP Report 598 RLT and AASHTO T 307 quick shear testing and one of three unique combinations of geogrid type and configuration, as applicable, for the CBR testing. The potential covariates were moisture content, as measured immediately after testing, and dry density, and they were represented in the ANOCOVA as percentage of OMC and percentage of MDD, respectively, where the OMC and MDD values

were those for the given aggregate base material. When either covariate had a p -value greater than 0.15, it was removed from the model. The p -value of 0.15 was used because it is the default value for variable selection using the stepwise function in the statistical analysis program used in this research (SAS 2010). The dependent variables were the modulus and number of cycles to failure from the NCHRP Report 598 testing; the peak axial stress, modulus to the peak stress, modulus of the elastic portion of the curve, and modulus at 2 percent strain from the AASHTO T 307 testing; and the CBR. For each dependent variable, post-hoc pairwise comparisons were performed to assess the difference between the control and each of the unique combinations of geogrid type and configuration that were evaluated. The differences were reported in terms of a t -value that facilitated comparison of the various treatment combinations. The treatment with the largest magnitude of t -value within any single subgroup of treatments was determined to be the most different from the control, where positive t -values signify an increase in structural capacity of the geogrid-reinforced specimens compared to the control specimens.

To determine which method of data analysis is most likely to consistently show an improvement in the structural capacity of geogrid-reinforced aggregate base materials, the lower bound of the 95 percent confidence interval for the t -values from the post-hoc pairwise comparisons that were performed on the results from the AASHTO T 307 testing was computed for each method of data analysis. In this analysis, the t -values for both aggregate base materials were pooled for each method, and an Anderson-Darling normality test was performed to determine if the pooled set of t -values for each method were normally distributed, where normal distributions are indicated by a p -value greater than or equal to 0.05. The data that were found to be non-normally distributed were transformed, as needed, and the Anderson-Darling normality test was performed again. The lower bound of the 95 percent confidence interval was then

computed for each method of data analysis by subtracting 1.96 standard deviations from the mean, where the mean and standard deviation were computed from the pooled set of t -values. For the method(s) for which a transformation was required, the resulting lower bound was then untransformed to give a value that could be directly compared to the other bounds. The method with the highest lower bound was determined to be the method most likely to show an improvement in structural capacity associated with geogrid reinforcement.

In addition, for the selected method of data analysis, to determine which geogrid configuration is most likely to consistently show an improvement in the structural capacity of geogrid-reinforced aggregate base materials, the lower bound of the 95 percent confidence interval for the t -values from the same post-hoc pairwise comparisons was computed. In this analysis, the t -values for both aggregate base materials were again pooled for each geogrid configuration, and an Anderson-Darling normality test was performed to determine if the data from each configuration were normally distributed. The lower bound of the 95 percent confidence interval was then computed for each configuration by subtracting 1.96 standard deviations from the mean, where the mean and standard deviation were computed from the pooled set of t -values. The geogrid configuration with the highest lower bound was determined to be the configuration most likely to show an improvement in structural capacity associated with geogrid reinforcement.

3.6 Summary

This research was motivated by the need to identify a single laboratory test protocol that UDOT engineers could specify to quantify improvements in structural capacity of aggregate base materials reinforced with geogrid. The factors investigated in this research were test protocol, aggregate base material, geogrid type, and geogrid placement. The testing protocols used in this

research were the NCHRP Report 598 RLT, AASHTO T 307 quick shear, and CBR protocols. Testing was performed on unreinforced and geogrid-reinforced aggregate base material from the Point of the Mountain Pit and the Trenton Gravel Pit #3, both of which are located in northern Utah. These materials were included in this research because they are representative of aggregate base materials commonly used on UDOT projects and because they also exhibit different particle angularity. Two geogrid types, BX and TX, were utilized in this research to ensure that the experimentation was representative of the geogrid products available in the industry. Three different reinforcement configurations were tested for each unique combination of aggregate and geogrid using the NCHRP Report 598 and AASHTO T 307 test protocols. Only one reinforcement configuration was used in CBR testing due to the reduced height of the specimens. Two replicates of each configuration were tested to allow for statistical analysis of the results.

The aggregate base materials used in this research were characterized using washed sieve analyses and Atterberg limits testing, and soil classifications were determined according to the USCS and AASHTO methods. The OMC and MDD were also determined.

The resilient modulus and number of cycles to failure were recorded for each specimen tested using the NCHRP Report 598 procedures. For the AASHTO T 307 testing, the resulting stress-strain plot for each specimen was analyzed, the peak axial stress was determined, and various modulus values were calculated from the plot, including the modulus to the peak axial stress, the modulus of the elastic portion of the curve, and the modulus at 2 percent strain in the specimens. The CBR was determined by dividing the measured stresses by the standard stresses and selecting the largest ratio. The dry density of each specimen was estimated from the wet density measured immediately after compaction and the moisture content measured immediately after testing.

An ANOCOVA was performed on the results of each test for each aggregate base material. For each dependent variable, post-hoc pairwise comparisons were performed, and t -values were calculated to assess the difference between the control and each of the unique treatment combinations of geogrid type and configuration that were evaluated. Anderson-Darling normality tests were performed to determine if the pooled sets of t -values were normally distributed, and the lower bounds of the 95 percent confidence intervals were computed. The test method and the geogrid configuration with the highest lower bound were determined to be the method and the configuration most likely to show an improvement in structural capacity associated with geogrid reinforcement.

4 RESULTS AND ANALYSIS

4.1 Overview

This chapter presents the results of testing and statistical analyses performed for this research. While the various laboratory test procedures are directly compared through formal statistical analyses, differences in performance between the two aggregate base materials and the two geogrid types are discussed only incidentally. As explained in Chapter 3, the two aggregate base materials and the two geogrid types were selected only to ensure that the experimentation was representative of the products available in the industry.

4.2 Test Results

Materials characterization included washed sieve analysis, Atterberg limits testing, soil classification, and determination of OMC and MDD for each aggregate base material. The results of the washed sieve analyses are plotted in Figure 4-1, which shows that the Point of the Mountain material is finer than the Trenton material. Based on the washed sieve analyses and the Atterberg limits testing, which indicated that neither material was plastic, the Point of the Mountain material was classified as A-1-a and SW-SM (well-graded sand with silt and gravel), and the Trenton material was classified as A-1-a and GW (well-graded gravel with sand) according to the AASHTO and USCS methods, respectively. The OMC and MDD values obtained from moisture-density testing of the materials are shown in Table 4-1, and the

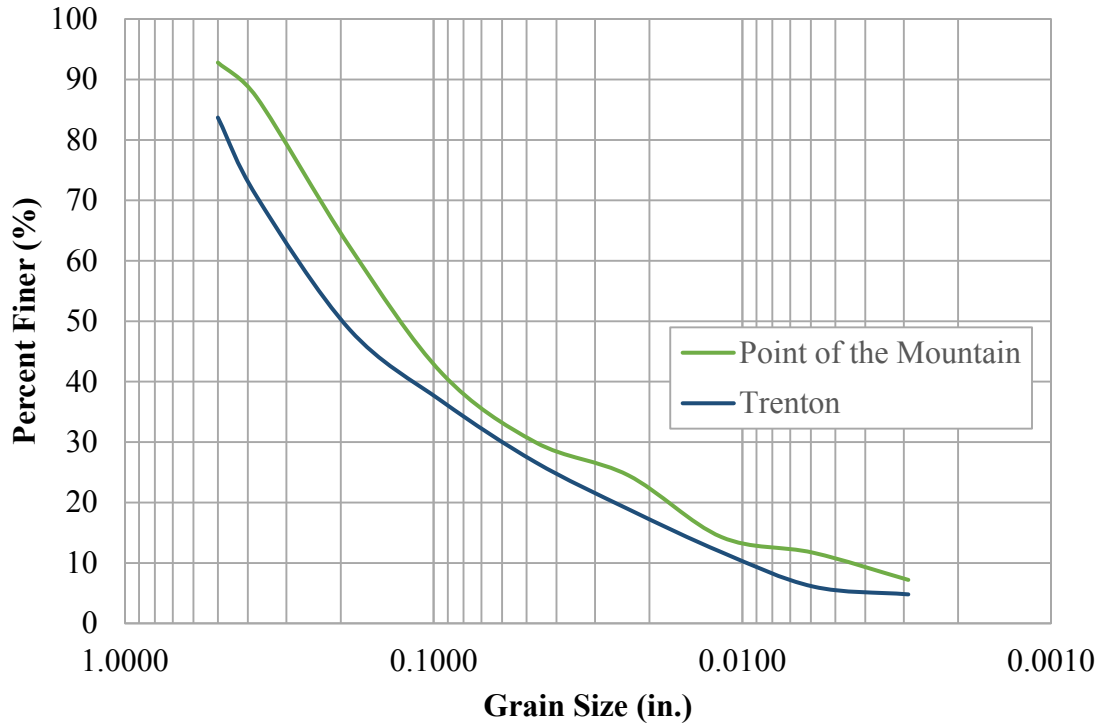


Figure 4-1: Particle-size distributions.

Table 4-1: Moisture-Density Relationships

Material	Optimum Moisture Content (%)	Maximum Dry Density (pcf)
Point of the Mountain	6.6	138.0
Trenton	5.6	142.2

corresponding moisture-density curves are shown in Appendix A. Given the relative sizes of the largest aggregate particles and the geogrid apertures, the results of especially the sieve analyses indicate that both aggregate base materials exhibit the potential for interlocking with both types of geogrid included in the study. Compared to the unreinforced condition, some improvement in structural capacity associated with geogrid reinforcement was therefore expected.

The average test results obtained in the NCHRP Report 598 RLT, AASHTO T 307 quick shear, and CBR tests are given in Tables 4-2 to 4-4, respectively; two replicate specimens were evaluated in each test. Hyphens in these tables indicate that geogrid configuration was not applicable due to the absence of geogrid in the control specimens. Data for individual specimens, including the moisture content measured immediately after testing and the estimated dry density, are provided in Appendix B. The results of statistical analyses and discussion of the data are provided in the next section.

Table 4-2: NCHRP Report 598 RLT Test Results

Material	Geogrid Type	Geogrid Configuration	Average Resilient Modulus (ksi)	Average Cycles to Failure
Point of the Mountain	None	-	23.3	7013
		A	20.9	6035
		B	21.7	6062
	BX	C	20.1	6230
		A	29.7	9926
		B	23.1	6797
TX	C	23.2	7177	
	None	-	29.0	7722
	A	26.9	7709	
Trenton	BX	B	27.3	8309
		C	21.9	5677
		A	35.4	9507
	TX	B	20.1	4583
		C	22.6	5382

Table 4-3: AASHTO T 307 Quick Shear Test Results

Material	Geogrid Type	Geogrid Configuration	Average Peak Axial Stress (psi)	Average Modulus to Peak Stress (psi)	Average Elastic Modulus (psi)	Average Modulus at 2% Strain (psi)	
Point of the Mountain	None	-	77.9	2591	3198	3414	
		A	97.3	3616	5352	4417	
		B	98.8	2998	3635	4081	
	BX	C	81.8	3617	5548	4203	
		A	83.8	2956	4783	3860	
		B	89.6	3064	4868	4143	
	TX	C	92.7	3963	5696	4436	
		None	-	55.5	575	965	874
		A	68.5	925	1089	1099	
Trenton	BX	B	84.9	609	1227	1145	
		C	58.8	1082	1228	1187	
		A	70.7	702	1137	1174	
	TX	B	86.9	704	1191	1183	
		C	49.1	845	1090	1071	

Table 4-4: CBR Test Results

Material	Geogrid Type	Geogrid Configuration	Average CBR
Point of the Mountain	None	-	109
	BX	A	142
	TX	A	94
Trenton	None	-	73
	BX	A	57
	TX	A	58

4.3 Statistical Analyses

The results of statistical analyses included results for the ANOCOVAs and also for post-hoc pairwise comparisons that were performed on the data. The p -values for the full and reduced ANOCOVA models are presented in Appendix C. Among the ANOCOVAs performed for the

Point of the Mountain material, moisture content was included as a covariate in terms of percentage of OMC in the analysis of the resilient modulus and cycles to failure data from the NCHRP Report 598 RLT testing, and dry density was included as a covariate in terms of percentage of MDD in the analysis of the peak axial stress data from the AASHTO T 307 quick shear testing. Among the ANOCOVAs performed for the Trenton material, neither moisture content nor dry density were included as covariates. The results of the post-hoc pairwise comparisons used to analyze the NCHRP Report 598, AASHTO T 307, and CBR test data are presented in Tables 4-5 through 4-7.

As shown in Tables 4-5 and 4-7, the average *t*-value calculated for both materials, both geogrid types, and all configurations from the NCHRP Report 598 and CBR testing is negative for each test result, signifying that the geogrid-reinforced specimens had lower structural

Table 4-5: Statistical Analyses of NCHRP Report 598 RLT Test Results

Material	Geogrid Type	Geogrid Configuration	<i>t</i> -value	
			Resilient Modulus	Cycles to Failure
Point of the Mountain	BX	A	-1.82	-1.89
		B	-2.09	-2.75
		C	-2.72	-1.77
	TX	A	4.78	5.44
		B	0.26	0.03
		C	1.86	2.45
Trenton	BX	A	-0.84	-0.01
		B	-0.68	0.53
		C	-2.83	-1.86
	TX	A	2.57	1.62
		B	-3.58	-2.85
		C	-2.56	-2.13
Average			-0.64	-0.27
Standard Deviation			2.44	2.38

Table 4-6: Statistical Analyses of AASHTO T 307 Quick Shear Test Results

Material	Geogrid Type	Geogrid Configuration	<i>t</i> -value			
			Peak Axial Stress	Modulus to Peak Stress	Elastic Modulus	Modulus at 2% Strain
Point of the Mountain	BX	A	0.61	1.94	2.27	2.46
		B	1.39	0.77	0.79	1.64
		C	-1.02	1.94	2.63	1.94
	TX	A	-0.52	0.69	1.50	1.10
		B	0.01	0.90	0.97	1.79
		C	-0.15	2.60	2.60	2.51
Trenton	BX	A	2.48	4.97	1.28	1.90
		B	5.56	0.47	2.35	2.28
		C	0.63	7.20	1.69	2.64
	TX	A	2.88	1.81	0.81	2.53
		B	5.95	1.83	1.87	2.60
		C	-1.20	3.83	1.17	1.66
Average			1.39	2.41	1.66	2.09
Standard Deviation			2.30	1.92	0.65	0.47

Table 4-7: Statistical Analyses of CBR Test Results

Material	Geogrid Type	Geogrid Configuration	<i>t</i> -value
			CBR
Point of the Mountain	BX	A	2.65
	TX	A	-1.24
Trenton	BX	A	-1.43
	TX	A	-1.32
Average			-0.34
Standard Deviation			1.72

capacity than the unreinforced specimens for both materials evaluated in this research according to those methods. Therefore, for the base materials and reinforcement configurations tested, the NCHRP Report 598 and CBR procedures are not likely to produce results showing an

improvement in resilient modulus, cycles to failure, or CBR as a result of the inclusion of geogrid in the test specimens; in particular, the results of the NCHRP Report 598 testing are consistent with selected literature showing that the inclusion of geogrid does not generally have a significant effect on the resilient modulus of base materials (Abu-Farsakh et al. 2012, Moghaddas-Nejad and Small 2003, Nazzal et al. 2007, Perkins et al. 2004, Wayne et al. 2011b). Because neither of these two test methods yielded results that satisfied the research objective, they are not discussed further.

As shown in Table 4-6, the average *t*-value calculated for both materials, both geogrid types, and all configuration from the AASHTO T 307 testing is positive for each method of data analysis, signifying that the geogrid-reinforced specimens had higher structural capacity than the unreinforced specimens for both materials evaluated in this research according to those methods. Therefore, for the base materials and reinforcement configurations tested, the AASHTO T 307 procedure is likely to produce results showing an improvement in peak axial stress, modulus to peak stress, elastic modulus, and/or modulus at 2 percent strain as a result of the inclusion of geogrid in the test specimens.

In the process of determining which method of data analysis is most likely to consistently show an improvement in the structural capacity of geogrid-reinforced specimens evaluated using the AASHTO T 307 procedure, use of the Anderson-Darling normality test showed that the peak axial stress, elastic modulus, and modulus at 2 percent strain data were normally distributed, while the modulus to peak stress data were not normally distributed; therefore, a square-root transformation was applied to normalize the modulus to peak stress data prior to computing the lower bound of the 95 percent confidence interval, which was then untransformed afterwards. The results showing the lower bound of the 95 percent confidence interval for each method of

data analysis are given in Table 4-8. Because the modulus at 2 percent strain had the highest lower bound of the 95 percent confidence interval, this method of data analysis was determined to be more likely than the other methods to consistently show an improvement in structural capacity associated with geogrid reinforcement.

In the process of determining which geogrid configuration is most likely to consistently show an improvement in the structural capacity of geogrid-reinforced specimens evaluated in terms of modulus at 2 percent strain using the AASHTO T 307 procedure, use of the Anderson-Darling normality test showed that the data for each of the three geogrid configurations were normally distributed. The results showing the lower bound of the 95 percent confidence interval for each geogrid configuration are shown in Table 4-9. Because the lower bounds of the 95 percent confidence intervals for configurations B and C were higher than that for configuration A and were also nearly equal to each other, configurations B and C were determined to be more likely than configuration A to consistently show an improvement in structural capacity

Table 4-8: Lower Bounds for AASHTO T 307 Methods of Data Analysis

	<i>t</i> -value			
	Peak Axial Stress	Modulus to Peak Stress	Elastic Modulus	Modulus at 2% Strain
Lower Bound	-3.12	0.10	0.39	1.17

Table 4-9: Lower Bounds for AASHTO T 307 Geogrid Configurations

	<i>t</i> -value		
	Configuration		
	A	B	C
Lower Bound	0.87	1.32	1.40

associated with geogrid reinforcement. (Another reason for not recommending configuration A is the difficulty associated with keeping a geogrid circle flat and horizontal, which is required to obtain repeatable results, while compacting it in the middle of a lift as required in configuration A.) Among configurations B and C, configuration B may be more favorable because specimens are more commonly reinforced at the middle, as evidenced in the literature (Perkins et al. 2004, Rahman et al. 2014, Wayne et al. 2011a). However, this research and previous research suggest that placing the geogrid at an upper position within a specimen, similar to configuration C, can yield a greater improvement in structural capacity than placing geogrid in the middle of the specimens (Abu-Farsakh et al. 2012, Nazzal et al. 2007).

The region of failure within the specimens, as evidenced by “barreling,” varied depending on the presence of geogrid and the geogrid configuration. Photographs illustrating the barreling behavior of specimens in the unreinforced condition and with each reinforcement configuration are shown in Figures 4-2 and 4-3 for the Point of the Mountain and Trenton materials, respectively. As observed in both materials, the region of barreling in the control specimens was not centered at the middle but was shifted slightly upwards from the middle, perhaps due to the development of a density gradient during compaction, where lower density may have occurred near the top of the specimen compared to the bottom of the specimen as observed in other research (Sebesta et al. 2004, NCHRP 2004b); for unreinforced specimens of uniform density, the region of barreling would be expected to occur in the middle. The region of barreling in the specimens reinforced with geogrid in configurations A and B was consistently above the geogrid in the region of possible lower density. The specimens reinforced with geogrid in configuration C failed in the region below the geogrid. These specimens likely did not fail in the region above the geogrid, which may have had lower density, due to the reinforcing effect of



(a)



(b)



(c)



(d)

Figure 4-2: Typical Point of the Mountain specimens after AASHTO T 307 quick shear testing: (a) no geogrid, (b) geogrid configuration A, (c) geogrid configuration B, (d) geogrid configuration C.



(a)



(b)



(c)



(d)

Figure 4-3: Typical Trenton specimens after AASHTO T 307 quick shear testing: (a) no geogrid, (b) geogrid configuration A, (c) geogrid configuration B, (d) geogrid configuration C.

the geogrid; previous research suggests that, in RLT testing, the influence of the geogrid extends approximately one specimen radius above and below the geogrid layer (Perkins et al. 2004). For configuration C in this research, the geogrid circles were placed 3 in. below the top surface of the aggregate base specimens, and, as a result, if the region influenced by the geogrid in quick shear testing is similar to that in RLT testing, the confinement provided by the geogrid would extend to the top surface of the specimens and would then not allow failure to occur in that region. Instead, failure would occur in the region of possible higher density below the geogrid, yielding a greater improvement in structural capacity compared to other configurations. For this reason, placing the geogrid at an upper position within a specimen, similar to configuration C, may be more useful for quantifying improvements in structural capacity of aggregate base materials reinforced with geogrid.

The results for configurations A, B, and C of geogrid-reinforced specimens evaluated in terms of modulus at 2 percent strain using the AASHTO T 307 procedure are shown in Figures 4-4 to 4-6, respectively. In each figure, for both the Point of the Mountain and Trenton materials, the percent increase in structural capacity associated with geogrid reinforcement compared to the unreinforced condition is given for both the BX and TX geogrid types. Although the modulus of the unreinforced Trenton specimens was 25.6 percent lower than that of the unreinforced Point of the Mountain specimens, which is probably attributable to the differences in angularity between the two materials, Figures 4-4 to 4-6 show that both types of geogrid provided substantial improvements in modulus compared to the control specimens; depending on geogrid configuration, the Point of the Mountain material experienced an improvement in modulus ranging from 13 to 30 percent, and the Trenton material experienced an improvement in modulus ranging from 23 to 36 percent.

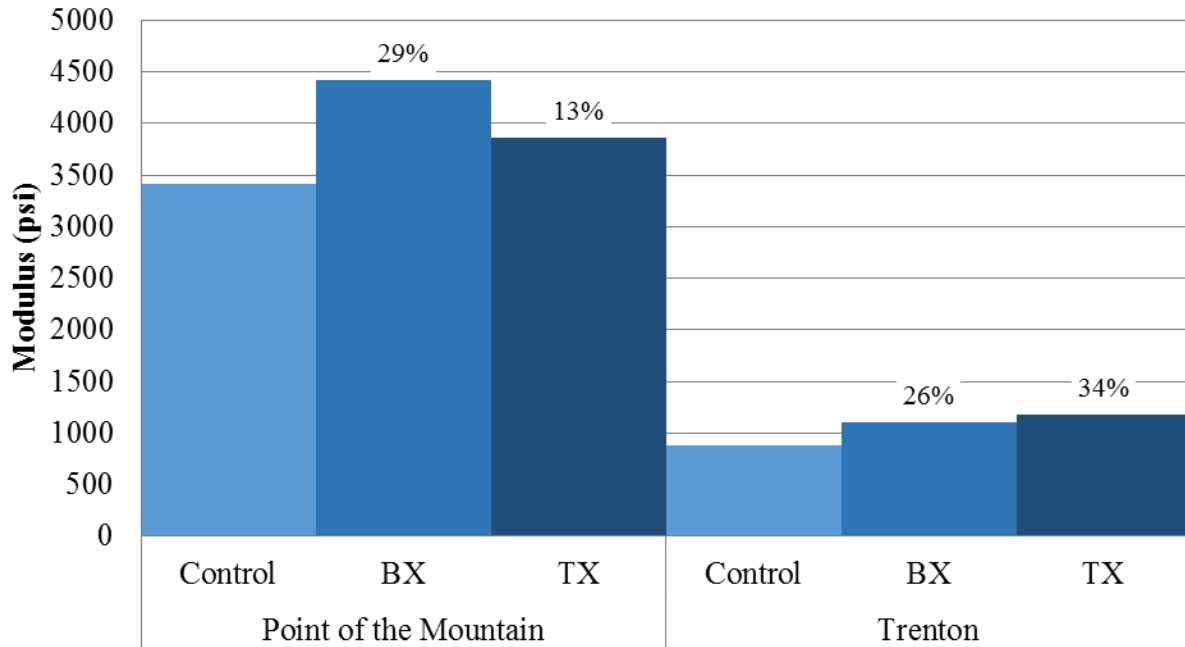


Figure 4-4: Modulus values for AASHTO T 307 quick shear testing in geogrid configuration A.

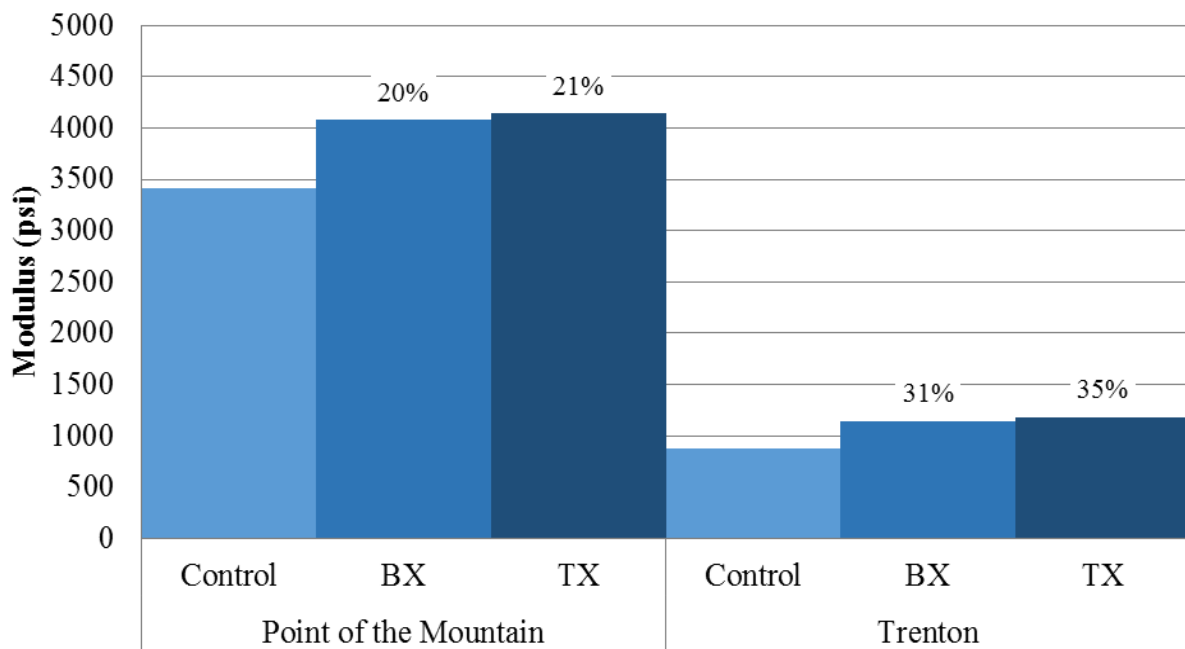


Figure 4-5: Modulus values for AASHTO T 307 quick shear testing in geogrid configuration B.

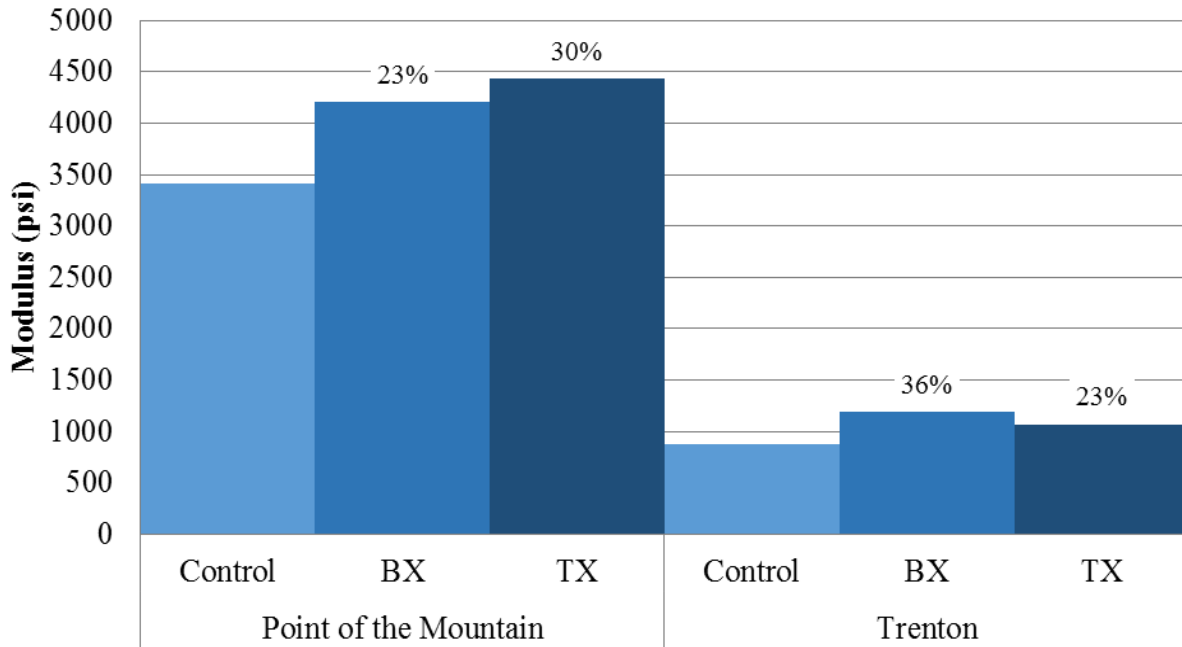


Figure 4-6: Modulus values for AASHTO T 307 quick shear testing in geogrid configuration C.

4.4 Summary

Based on the washed sieve analyses and the Atterberg limits testing, which indicated that neither material was plastic, the Point of the Mountain material was classified as A-1-a and SW-SM (well-graded sand with silt and gravel), and the Trenton material was classified as A-1-a and GW (well-graded gravel with sand) according to the AASHTO and USCS methods, respectively. The OMC and MDD values were 6.6 percent and 138.0 pcf for the Point of the Mountain material and 5.6 percent and 142.2 pcf for the Trenton material. Given the relative sizes of the largest aggregate particles and the geogrid apertures, the results of especially the sieve analyses indicate that both aggregate base materials exhibit the potential for interlocking with both types of geogrid included in the study. Compared to the unreinforced condition, some improvement in structural capacity associated with geogrid reinforcement was therefore expected.

For the methods and materials evaluated in this study, the average t -values from the post-hoc pairwise comparisons for the NCHRP Report 598 RLT and CBR testing were negative for each test result, signifying that the geogrid-reinforced specimens had lower structural capacity than the unreinforced specimens for both materials evaluated in this research according to those methods. The average t -values from the post-hoc pairwise comparisons for the AASHTO T 307 quick shear testing were positive for each method of data analysis, signifying that the geogrid-reinforced specimens had higher structural capacity than the unreinforced specimens for both materials evaluated in this research according to those methods.

Use of the Anderson-Darling normality test on the results of each of the four methods of data analysis for AASHTO T 307 showed that only the modulus to peak stress data were not normally distributed; therefore, a square-root transformation was applied to normalize this data prior to computing the lower bound of the 95 percent confidence interval, which was then untransformed afterwards. Because the modulus at 2 percent strain had the highest lower bound of the 95 percent confidence interval, this method of data analysis was determined to be more likely than the other methods to consistently show an improvement in structural capacity associated with geogrid reinforcement.

Use of the Anderson-Darling normality test on the modulus at 2 percent strain data from the AASHTO T 307 procedure showed that the data for each of the three geogrid configurations were normally distributed. Because the lower bounds of the 95 percent confidence intervals for configurations B and C were higher than that for configuration A and were also nearly equal to each other, configurations B and C were determined to be more likely than configuration A to consistently show an improvement in structural capacity. Among configurations B and C, configuration B may be more favorable because specimens are more commonly reinforced at the

middle, as evidenced in the literature. However, this research and previous research suggests that placing the geogrid at an upper position within a specimen, similar to configuration C, can yield a greater improvement in structural capacity than placing geogrid in the middle of the specimens.

For the protocols and geogrid configurations evaluated in this research, both types of geogrid provided substantial improvements in modulus for the geogrid-reinforced specimens when compared to the control specimens. Depending on geogrid configuration, the Point of the Mountain material experienced an improvement in modulus ranging from 13 to 30 percent, and the Trenton material experienced an improvement in modulus ranging from 23 to 36 percent.

5 CONCLUSION

5.1 Summary

The modulus of aggregate base layers in pavement structures can potentially be increased through the use of geogrid. To the extent that the aggregate particles penetrate the openings in the geogrid, the geogrid increases the lateral confinement of the base material in the region around the geogrid, which can result in an increase in the modulus of the base layer. However, methods for determining how much structural benefit can be expected from a given geogrid product have not been standardized. A laboratory testing protocol is therefore needed to enable evaluation, in terms of modulus or CBR, for example, of the degree of improvement that may be achieved by a given geogrid so that the cost of incorporating the geogrid in a pavement structure can be compared with the potential cost savings associated with its use. Consequently, the objective of this research was to identify a laboratory test method that can be used to quantify improvements in structural capacity associated with geogrid reinforcement.

For this research, NCHRP Report 598 RLT, AASHTO T 307 quick shear, and CBR testing protocols were used to test unreinforced and geogrid-reinforced aggregate base materials from the Point of the Mountain Pit and the Trenton Gravel Pit #3, both of which are located in northern Utah. These materials were included in this research because they are representative of aggregate base materials commonly used on UDOT projects and because they also exhibit different particle angularity. Two geogrid types, BX and TX, were utilized in this research to

ensure that the experimentation was representative of the geogrid products available in the industry. Three different reinforcement configurations were tested for each unique combination of aggregate and geogrid using the NCHRP Report 598 and AASHTO T 307 test protocols. Only one reinforcement configuration was used in CBR testing due to the reduced height of the specimens. Two replicates of each configuration were tested to allow for statistical analyses of the results. Several statistical analyses were performed on the results of each test method to identify the test that is most likely to consistently show an improvement in the structural capacity of aggregate base materials reinforced with geogrid.

5.2 Findings

The results of this research indicate that, for the methods and materials evaluated in this study, the NCHRP Report 598 RLT and CBR test methods are not likely to show an improvement in structural capacity associated with geogrid reinforcement. Instead, calculation of the modulus at 2 percent strain from the AASHTO T 307 quick shear data is the method most likely to consistently show an improvement in structural capacity associated with geogrid reinforcement. Among the three configurations investigated as part of this research, configuration C, with geogrid placed at an upper position within a specimen, is preferred over configurations A and B.

5.3 Recommendations

Calculation of the modulus at 2 percent strain from the AASHTO T 307 quick shear data is recommended as a laboratory test protocol that engineers can specify to quantify improvements in structural capacity of aggregate base materials reinforced with geogrid. Placing the geogrid at an upper position within a specimen, similar to configuration C, is recommended

as the configuration most likely to show an improvement in structural capacity associated with geogrid reinforcement.

Given that the end goal of the use of geogrid reinforcement is to improve pavement performance, additional research is needed to compare the results of the AASHTO T 307 quick shear test obtained in the laboratory with the structural capacity of geogrid-reinforced aggregate base materials measured in the field. In addition, correlations between the results of the AASHTO T 307 quick shear test and resilient modulus need to be investigated in order to incorporate the findings of the AASHTO T 307 quick shear test on reinforced base materials into mechanistic-empirical pavement design; similar correlations for unreinforced base materials have already been developed (Hossain 2008). Finally, other combinations of aggregate base material and geogrid should be evaluated using the AASHTO T 307 quick shear test to determine the degree to which improvements in modulus of aggregate base materials reinforced with geogrid can be assessed.

REFERENCES

- Abu-Farsakh, M., Souci, G., Voyiadjis, G. Z., and Chen, Q. (2012). "Evaluation of factors affecting the performance of geogrid-reinforced granular base material using repeated load triaxial tests." *Journal of Materials in Civil Engineering*, 24(1), 72-83.
- Al-Qadi, I. L., Brandon, T. L., and Bhutta, S. A. (1997). "Geosynthetic stabilized flexible pavements." *Proceedings of Geosynthetics '97*, Industrial Fabrics Association International (IFAI), Roseville, MN, 647-662.
- Al-Qadi, I. L., Dessouky, S. H., Kwon, J., and Tutumluer, E. (2008). "Geogrid in flexible pavements: validated mechanism." *Transportation Research Record: Journal of the Transportation Research Board*, 2045, 102-109.
- American Association of State Highway and Transportation Officials (AASHTO) (2008). "Mechanistic-empirical pavement design guide: a manual of practice." Washington, DC.
- Brown, S. F., Kwan, J., and Thom, N. H. (2007). "Identifying the key parameters that influence geogrid reinforcement of railway ballast." *Geotextiles and Geomembranes*, 25(6), 326-335.
- Cancelli, A., and Montanelli, F. (1999). "In-ground test for geosynthetic reinforced flexible paved roads." *Proceedings of the Conference Geosynthetics '99*, IFAI, Roseville, MN, 863-878.
- Chen, Q., and Abu-Farsakh, M. (2012). "Structural contribution of geogrid reinforcement in pavement." *GeoCongress 2012: State of the Art and Practice in Geotechnical Engineering*, ASCE, Reston, VA, 1468-1475.
- Hatami, K., Mahmood, T., Zaman, M., and Ghabchi, R. (2012). "Development of ODOT guidelines for the use of geogrids in aggregate bases." Report No. OTCREOS9.1-23-F, Oklahoma Transportation Center, Midwest City, OK.

- Hossain, M. S. (2008). "Characterization of subgrade resilient modulus for Virginia soils and its correlation with the results of other soil tests." Report No. VTRC 09-R4, Virginia Transportation Research Council, Charlottesville, VA.
- Jackson, K. (2015). "Laboratory resilient modulus measurements of aggregate base materials in Utah." M.S. thesis, Department of Civil and Environmental Engineering, Brigham Young University, Provo, UT.
- Kwon, J., Tutumluer, E., Al-Qadi, I., and Dessouky, S. (2008). "Effectiveness of geogrid base-reinforcement in low-volume flexible pavements." *GeoCongress 2008: Geosustainability and Geohazard Mitigation*, ASCE, Reston, VA.
- Kwon, J., and Tutumluer, E. (2009). "Geogrid base reinforcement with aggregate interlock and modeling of associated stiffness enhancement in mechanistic pavement analysis." *Transportation Research Record: Journal of the Transportation Research Board*, 2116, 85-95.
- Moghaddas-Nejad, F., and Small, J. C. (2003). "Resilient and permanent characteristics of reinforced granular materials by repeated load triaxial tests." *Geotechnical Testing Journal*, 26(2), 152-166.
- Montanelli, F., Zhao, A., and Rimoldi, P. (1997). "Geosynthetic-reinforced pavement system: testing and design." *Proceedings of the Conference Geosynthetics '97*, IFAI, Roseville, MN, 619-632.
- Nazzal, M., Abu-Farsakh, M., and Mohammad, L. (2007). "Evaluation of geogrid benefits using monotonic and repeated load triaxial tests." *Analysis of Asphalt Pavement Materials and Systems*, 145-155.
- National Cooperative Highway Research Program (NCHRP) (2004a). "Guide for mechanistic-empirical design of new and rehabilitated structures." NCHRP Report 1-37A, Transportation Research Board, Washington, DC.
- NCHRP (2004b). "Laboratory determination of resilient modulus for flexible pavement design." NCHRP Report 1-28A, Transportation Research Board, Washington, DC.
- National Highway Institute (NHI) (2002). "Introduction to mechanistic-empirical pavement design: reference manual." NHI-02-048, Arlington, VA.
- Palmeira, E. M. (2004). "Bearing force mobilisation in pull-out tests on geogrids." *Geotextiles and Geomembranes*, 22(6), 481-509.

- Perkins, S. W., and Ismeik, M. A. (1997). "A synthesis and evaluation of geosynthetic-reinforced base layers in flexible pavements: part I. *Geosynthetics International*, (4)6, 549-604.
- Perkins, S. W. (1999). "Geosynthetic reinforcement of flexible pavements: laboratory based pavement test sections." Report No. FHWA/MT-99-001/8138, Federal Highway Administration, Washington, DC.
- Perkins, S. W., Christopher, B. R., Cuelho, E. L., Eiksund, G. R., Hoff, I., Schwartz, C. W., Svanø, G., and Watn, A. (2004). "Development of design methods for geosynthetic-reinforced flexible pavements." Report No. DTFH61-01-X-00068, U.S. Dept. of Transportation, Federal Highway Administration, Washington, DC.
- Qian, Y., Han, J., Pokharel, S., and Parsons, R. (2013). "Performance of triangular aperture geogrid-reinforced base courses over weak subgrade under cyclic loading." *Journal of Materials in Civil Engineering*, 25(8), 1013-1021.
- Rahman, M., Arulrajah, A., Piratheepan, J., Bo, M., and Imteaz, M. (2014). "Resilient modulus and permanent deformation responses of geogrid-reinforced construction and demolition materials." *Journal of Materials in Civil Engineering*, 26(3), 512-519.
- SAS. (2010). Version 9.3, SAS Institute, Inc., Cary, NC.
- Sebesta, S., Guthrie, W. S., and Harris, J. P. (2004). "Gyratory compaction of soils for laboratory swell tests." *Transportation Research Board 83rd Annual Meeting*, Washington, DC.
- Tang, X., Stoffels, S. M., and Palomino, A. M. (2013). "Resilient and permanent deformation characteristics of unbound pavement layers modified by geogrids." *Transportation Research Record: Journal of the Transportation Research Board*, 2369, 3-10.
- Tutumluer, E., and Kwon, J. (2006). "Evaluation of geosynthetics use for pavement subgrade restraint and working platform construction." *ASCE Geotechnical Practice Publication No. 3: Geotechnical Applications for Transportation Infrastructure*, Titi, H., eds., ASCE, Reston, VA, 96-107.
- Tutumluer, E., Huang, H., and Bian, X. (2009). "Research on the behaviour of geogrids in stabilisation applications." *Proceedings of Jubilee Symposium on Polymer Geogrid Reinforcement*, Tensar International Limited, Blackburn, UK.
- Wayne, M., Boudreau R. L., and Kwon, J. (2011a). "Characterization of mechanically stabilized layer by resilient modulus and permanent deformation testing. *Transportation Research Record: Journal of the Transportation Research Board*, 2204, 76-82.

Wayne, M. H., Kwon, J., and Boudreau, R. (2011b). “Resilient modulus, repeated load permanent deformation and plate load testing of a mechanically stabilized crushed miscellaneous base material.” *Transportation Research Board 90th Annual Meeting*, Washington, DC.

Xiao, Y., Tutumluer, E., Qian, Y., and Siekmeier, J. A. (2012). “Gradation effects influencing mechanical properties of aggregate base-granular subbase materials in Minnesota.” *Transportation Research Record: Journal of the Transportation Research Board*, 2267, 14-26.

APPENDIX A MOISTURE-DENSITY RELATIONSHIPS

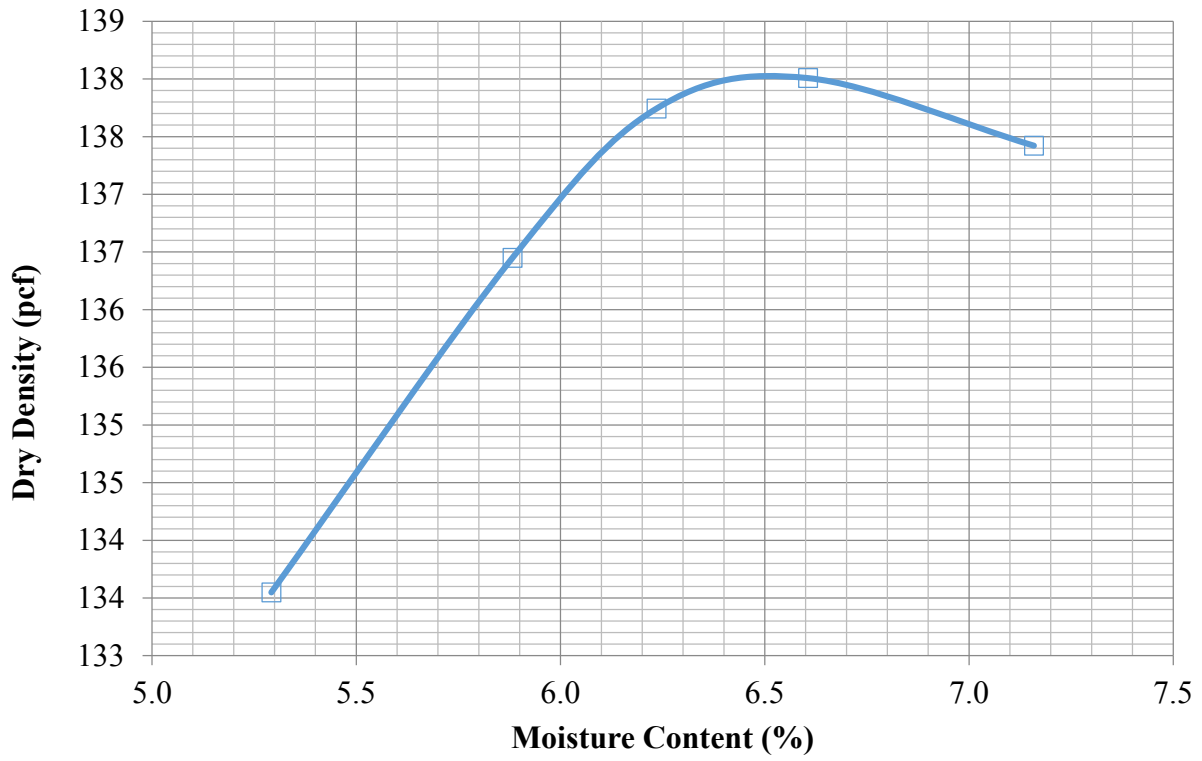


Figure A-1: Moisture-density curve for Point of the Mountain material.

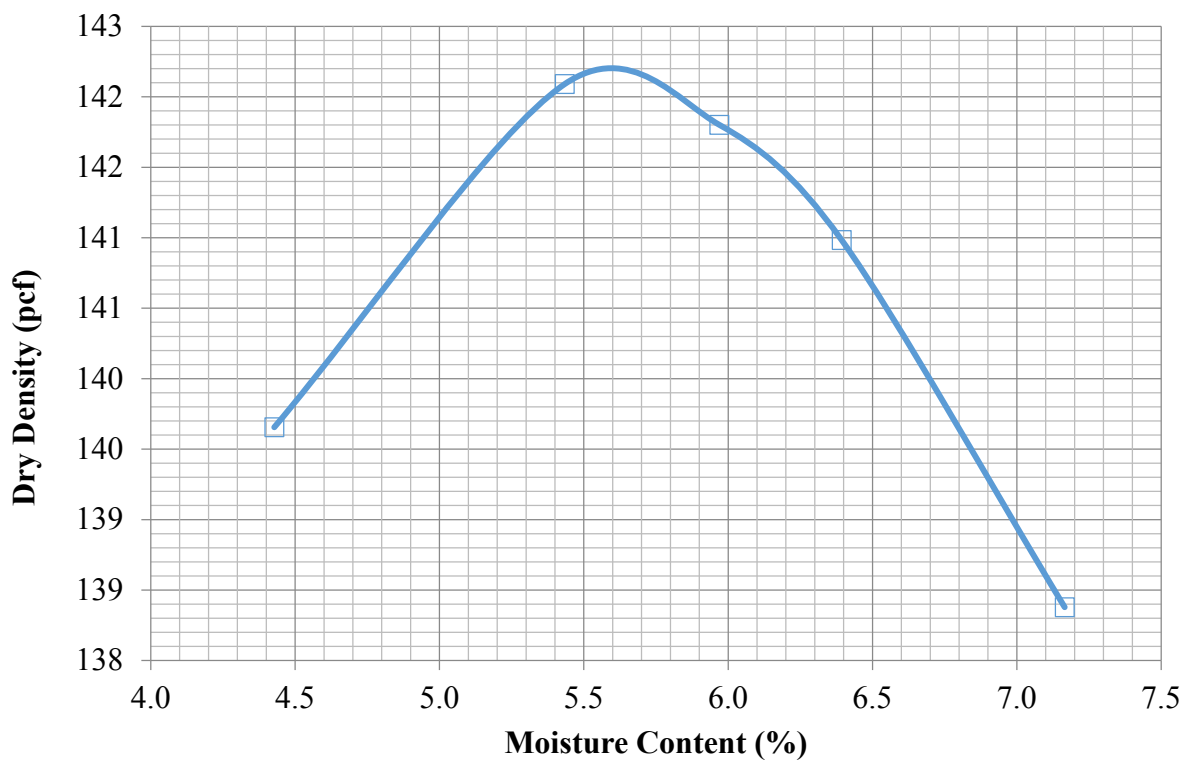


Figure A-2: Moisture-density curve for Trenton material.

APPENDIX B MECHANICAL PROPERTY TEST DATA

Table B-1: NCHRP Report 598 RLT Test Data

Material	Geogrid Type	Geogrid Configuration	Specimen	Height (in.)	Weight (lb)	Moisture Content (%)	Estimated Dry Density (pcf)	Resilient Modulus (ksi)	Cycles to Failure	
Point of the Mountain	None	-	1	11.66	28.36	6.0	137.2	25.6	8312	
			2	11.80	28.76	6.2	137.1	21.0	5714	
	BX	A	1	11.88	28.78	6.0	137.3	23.5	7014	
			2	11.82	28.80	6.2	137.2	18.4	5055	
		B	1	11.66	27.74	6.0	134.8	23.1	6757	
			2	11.82	28.75	6.1	138.3	20.3	5367	
	C	1	11.83	28.81	6.1	138.9	20.9	6360		
		2	11.82	28.81	6.0	137.8	19.2	6100		
	TX	A	1	11.94	28.77	6.1	135.3	29.7	9852	
			2	11.89	28.77	6.1	135.9	29.7	10000	
		B	1	11.79	28.80	6.1	138.4	22.6	6774	
			2	11.82	28.76	6.1	137.4	23.6	6820	
		C	1	11.81	28.81	6.3	137.5	21.4	6617	
			2	11.83	28.66	6.1	136.1	25.0	7736	
	Trenton	None	-	1	11.79	28.92	5.8	138.8	27.4	6955
				2	11.86	28.93	6.1	138.2	30.6	8489
		BX	A	1	11.80	28.93	5.9	140.5	25.0	6414
				2	11.88	28.90	6.1	140.6	28.8	9004
B			1	11.83	28.76	5.7	138.6	29.7	9325	
			2	11.87	28.94	5.8	139.4	24.9	7293	
C		1	11.83	28.91	6.0	139.8	23.1	6038		
		2	11.83	28.86	6.0	139.1	20.8	5316		
TX		A	1	11.79	28.71	5.5	138.6	37.3	10000	
			2	11.86	28.61	5.4	137.6	33.5	9013	
		B	1	11.85	28.86	6.2	138.3	21.9	5059	
			2	11.88	28.89	6.2	136.7	18.2	4107	
	C	1	11.82	28.97	6.4	137.6	24.0	5967		
		2	11.84	28.81	6.4	136.3	21.3	4796		

Table B-2: AASHTO T 307 Quick Shear Test Data

Material	Geogrid Type	Geogrid Configuration	Specimen	Height (in.)	Weight (lb)	Moisture Content (%)	Estimated Dry Density (pcf)	Peak Axial Stress (psi)	Modulus to Peak Stress (psi)	Modulus of Elastic Region (psi)	Modulus at 2% Strain (psi)
Point of the Mountain	None	-	1	11.81	28.81	6.8	136.0	88.9	2717	3112	3690
			2	11.80	28.81	6.7	139.1	67.0	2466	3266	3139
	BX	A	1	11.94	28.81	6.6	135.2	103.1	3699	4745	4491
			2	11.89	28.81	6.5	136.0	91.6	3532	4856	4343
		B	1	11.82	28.80	6.6	135.9	105.9	2676	3314	4143
			2	11.91	28.79	6.7	136.6	91.6	3319	4188	4019
	C	1	11.87	28.80	6.5	135.3	84.2	3785	5214	4466	
		2	11.83	28.79	6.4	136.1	79.5	3449	4901	3940	
	TX	A	1	11.81	28.81	6.5	136.1	75.9	2275	3287	3271
			2	11.83	28.81	6.6	136.1	91.7	3636	5221	4450
		B	1	11.84	28.81	6.6	136.2	95.0	3473	4080	4334
			2	11.89	28.80	6.6	135.6	84.1	2655	3672	3951
		C	1	11.89	28.78	6.6	134.9	91.5	3527	4284	4228
			2	11.84	28.81	6.4	135.6	93.9	4399	5783	4644
Trenton	None	-	1	11.82	28.92	6.4	137.9	61.2	616	1046	950
			2	11.87	28.96	6.4	136.9	49.7	535	810	798
	BX	A	1	11.75	29.00	6.3	138.5	70.2	951	1238	1200
			2	11.81	29.00	6.2	139.0	66.9	899	959	999
		B	1	11.83	28.97	6.3	137.9	87.8	589	1193	1198
			2	11.78	28.97	6.3	139.1	82.0	629	1287	1092
	C	1	11.77	28.96	6.3	139.1	60.0	1099	1225	1330	
		2	11.79	28.94	6.2	138.6	57.6	1065	1079	1044	
	TX	A	1	11.67	28.91	6.2	140.0	65.3	785	1165	1117
			2	11.75	28.89	6.2	137.8	76.1	619	906	1231
		B	1	11.82	28.91	6.3	137.5	83.2	784	1172	1141
			2	11.77	28.90	6.3	138.1	90.6	624	1180	1224
		C	1	11.79	28.95	6.2	138.3	52.2	877	1147	999
			2	11.74	28.95	6.2	138.6	46.1	813	1021	1144

Table B-3: CBR Test Data

Material	Geogrid Type	Geogrid Configuration	Specimen	Height (in.)	Weight (lb)	Moisture Content (%)	Estimated Dry Density (psf)	CBR
Point of the Mountain	None	-	1	4.55	10.86	6.23	137.2	111
			2	4.53	10.92	6.20	138.5	107
	BX	A	1	4.68	10.98	6.30	134.3	134
			2	4.66	10.97	6.30	135.3	150
	TX	A	1	4.63	10.98	6.40	136.2	82
			2	4.66	10.98	6.35	135.2	107
Trenton	None	-	1	4.61	11.07	6.27	137.8	64
			2	4.59	11.05	6.24	138.1	82
	BX	A	1	4.67	11.12	6.42	135.7	63
			2	4.64	11.13	6.43	137.2	51
	TX	A	1	4.61	11.10	6.27	139.1	50
			2	4.66	11.12	6.35	136.6	67

APPENDIX C ANOCOVA RESULTS

The full and reduced models resulting from the ANOCOVA's performed in this research are presented in Tables C-1 and C-2. The full models include the independent variable of treatment and both potential covariates of moisture content and dry density. The reduced models include the independent variable of treatment and only the covariates having a p -value greater than 0.15. In these analyses, the null hypothesis was that the means of the levels of each independent variable or covariate were equal, and the alternative hypothesis was that at least one mean was different from another. When the p -values computed in the analysis are less than or equal to 0.05, the null hypothesis can be rejected, and the alternative hypothesis can be accepted. However, as the purpose of the ANOCOVA was only to adjust the test results for statistically significant covariates in preparation for the post-hoc pairwise comparisons that were performed to assess the difference between the control and each of the unique combinations of geogrid type and configuration that were evaluated, hypothesis testing was not performed. Indeed, the p -values shown in these models for treatment are probably not meaningful in the context of this research, as the comparatively small sample size used in this experimentation may prevent identification of statistically significant effects of geogrid reinforcement even when practically important differences are observed. When the results for all geogrid-reinforced specimens are pooled together for a given test and compared to the corresponding results for control specimens, more meaningful p -values are obtained as shown in Appendix D.

Table C-1: Full ANOCOVA Models

Material	Effect	<i>p</i> -value						
		NCHRP 598 RLT		AASHTO T 307 Quick Shear			CBR	
		Resilient Modulus	Cycles to Failure	Peak Axial Stress	Modulus to Peak Stress	Modulus of Elastic Region	Modulus at 2% Strain	CBR
Point of the Mountain	Moisture Content (% of OMC)	0.0190	0.0104	0.4865	0.5113	0.7287	0.4909	0.5416
	Dry Density (% of MDD)	0.5501	0.4492	0.1197	0.7460	0.5603	0.5992	0.8237
	Treatment	0.0211	0.0107	0.5101	0.6213	0.6787	0.8128	0.5895
Trenton	Moisture Content (% of OMC)	0.4718	0.2653	0.1824	0.6240	0.7179	0.5893	0.6713
	Dry Density (% of MDD)	0.3282	0.5413	0.2408	0.2420	0.1802	0.7201	0.4657
	Treatment	0.1247	0.2303	0.0031	0.0168	0.4685	0.6745	0.8912

Table C-2: Reduced ANOCOVA Models

Material	Effect	<i>p</i> -value						
		NCHRP 598 RLT		AASHTO T 307 Quick Shear			CBR	
		Resilient Modulus	Cycles to Failure	Peak Axial Stress	Modulus to Peak Stress	Modulus of Elastic Region	Modulus at 2% Strain	CBR
Point of the Mountain	Moisture Content (% of OMC)	0.0076	0.0043	-	-	-	-	-
	Dry Density (% of MDD)	-	-	0.0534	-	-	-	-
	Treatment	0.0031	0.0020	0.2670	0.2587	0.1867	0.3005	0.0641
Trenton	Moisture Content (% of OMC)	-	-	-	-	-	-	-
	Dry Density (% of MDD)	-	-	-	-	-	-	-
	Treatment	0.0057	0.0230	0.0011	0.0016	0.4137	0.2400	0.3991

APPENDIX D POST-HOC COMPARISONS OF MEANS

Different than the post-hoc pairwise comparisons that were performed to assess the difference between the control and each of the unique combinations of geogrid type and configuration that were evaluated in this research, the post-hoc comparisons reported in this appendix were performed to assess the difference between the control and all of the unique combinations of geogrid type and configuration pooled together. In this analysis, the null hypothesis was that the means of the test results for the unreinforced and reinforced specimens were equal, and the alternative hypothesis was that they were not equal. When the p -values computed in the analysis are less than or equal to 0.05, the null hypothesis can be rejected, and the alternative hypothesis can be accepted. As shown in Table D-1, the effects of geogrid reinforcement are statistically significant for many of the test results; however, the modulus at 2

Table D-1: Post-Hoc Comparisons of Means

Test Protocol	Result	p -value	
		Point of the Mountain	Trenton
NCHRP 598 RLT	Resilient Modulus	0.9192	0.1271
	Cycles to Failure	0.7096	0.3399
	Peak Axial Stress	0.9652	0.0092
AASHTO T 307 Quick Shear	Modulus to Peak Stress	0.0952	0.0032
	Modulus of Elastic Region	0.0512	0.0852
	Modulus at 2% Strain	0.0414	0.0207
CBR	CBR	0.4748	0.2104

percent strain is the only test result that yielded p -values less than or equal to 0.05 for both aggregate base materials.